



CrossMark
click for updates

Cite this: *RSC Adv.*, 2016, 6, 36705

Steric and chelating ring concerns on the L-lactide polymerization by asymmetric β -diketiminato zinc complexes†

Wan-Jung Chuang,^a Hsing-Yin Chen,^a Wei-Ting Chen,^a Heng-Yi Chang,^a Michael Y. Chiang,^{ab} Hsuan-Ying Chen^{*a} and Sodio C. N. Hsu^{*a}

A series of new asymmetrical *N*-aryl-*N'*-alkyl β -diketiminates bearing a pendant pyridyl group (L^1H-L^4H) were synthesized in a two steps reaction from acetylacetone and the corresponding appropriate amines. The reaction of these β -diketiminates (LH) with $ZnEt_2$ afforded the corresponding ethyl zinc complexes. The ethyl zinc complexes were characterized by NMR spectroscopy and single crystal X-ray diffraction to confirm their structure and ligand binding mode. Diffusion-ordered nuclear magnetic resonance spectroscopy (DOSY) experiments yielded diffusion coefficients suggesting that all ethyl zinc complexes are monomeric in solution. All these zinc complexes demonstrate catalytic capabilities towards the ring-opening polymerization of L-lactide. The rate of polymerization depended heavily on the ligand favoring steric bulky aryl substituents (1,3,5-trimethylphenyl) and short pendant arms (pyridylmethyl).

Received 22nd March 2016
Accepted 4th April 2016

DOI: 10.1039/c6ra07453g

www.rsc.org/advances

Introduction

Due to environmental concerns, petrolic plastics are gradually being replaced with biodegradable materials such as aliphatic polyester.¹ Polylactide (PLA), produced by the ring-opening polymerization (ROP) of lactide (LA),² is a leading biodegradable and biocompatible polyester, which has attracted considerable attention due to its suitability for biomedical and pharmaceutical applications.³ Zinc complexes bearing ligands including β -diketiminato,^{4–10} bis(imino)aryl NCN pincer,¹¹ bis(pyrazol-yl)methane-base NNO-donor scorpionate,¹² Schiff base,¹³ anilido-alimine,¹⁴ amido-oxazolinato,¹⁵ diimine,¹⁶ maltolate,¹⁷ and phosphido pincer ligand¹⁸ have proven to be efficient catalysts for the ROP of lactides. These ROP catalysts resulted in polymers with well-controlled molecular weight and narrow molecular weight distribution.

Zinc complexes bearing bidentate ligands with nitrogen donors have been extensively applied to the studies on ROP of lactides. The substituent effects of the polymerization of LA by zinc complexes bearing bidentate β -diketiminato ligands were previously studied by Coates *et al.*^{3,4} and the investigations on the electronic effects of the substituents on the electronic

properties of the *N*-aryl groups were examined by Lin *et al.*⁷ A few *NNN*-tridentate β -diketiminato zinc complexes have been reported in studies concerning the lactide ROP reaction.^{9,10} Chen reported the first asymmetric *NNN*-tridentate β -diketiminato zinc complex and implied the flexible pendant arm may affect ROP activity.⁹ Recently, an asymmetric *N*-aryl-*N'*-alkyl β -diketiminato zinc complex bearing pendant pyridyl group was shown to be a highly active and good catalyst in the ROP of LA.¹⁰ Despite the extensive studies previously, two important issues remain unanswered: (1) how the length of flexible pendant arm govern the zinc complexes formation and ROP activity? (2) Do the steric bulkiness of the substituents effect the polymerization result? To answer these questions, four different *N*-aryl-*N'*-alkyl β -diketiminato ligands bearing aryl substituents of different size or pendant pyridyl arm with different length (Chart 1) were designed and reported herein on their coordination behavior. Furthermore, we reported the synthesis of a series of zinc complexes ligated by these asymmetrical β -diketiminato ligands as well as their structure–reactivity relationship in the ROP of L-lactide.

Results and discussion

Ligand synthesis and characterization

2-((2,6-Diisopropylphenyl)imido)-2-penten-4-one and 2-((2,4,6-trimethylphenyl)imido)-2-penten-4-one were prepared by simple condensation of acetylacetone with an equimolar amount of corresponding aniline in the presence of a catalytic amount *p*-toluenesulfonic acid (TsOH) and water was removed azeotropically during the reaction. The products were subsequently treated with appropriate amine in toluene and in the

^aDepartment of Medicinal and Applied Chemistry, Kaohsiung Medical University, Kaohsiung 807, Taiwan. E-mail: hchen@kmu.edu.tw; sodiohsu@kmu.edu.tw; Fax: +886-7-3125339; Tel: +886-7-3121101-2585; +886-7-3121101-6984

^bDepartment of Chemistry, National Sun Yat-Sen University, Kaohsiung 804, Taiwan

† Electronic supplementary information (ESI) available: Text containing additional figures (Fig. S1–S30), tables (Tables S1 and S2), and crystallographic data in CIF format for the structure determinations of L^1H , zinc complexes 1–4. CCDC 1434846–1434850. For ESI and crystallographic data in CIF or other electronic format see DOI: 10.1039/c6ra07453g

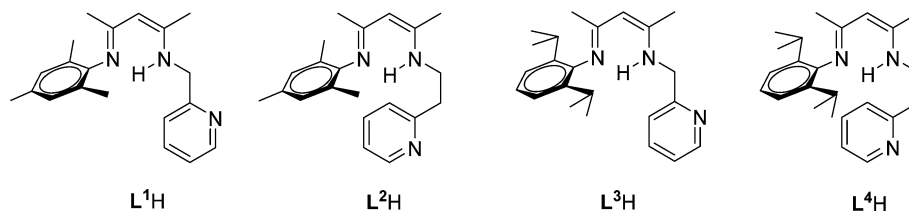
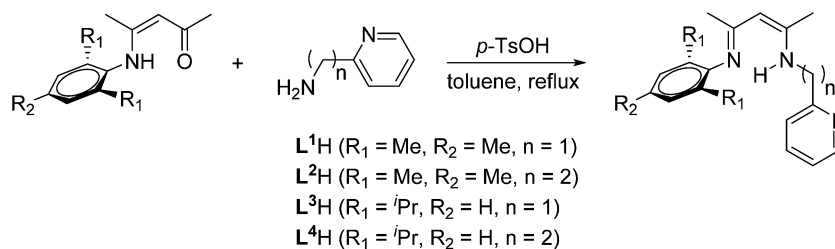


Chart 1 Representation of the *N*-aryl-*N'*-alkyl β -diketimine ligand sets.



Scheme 1 Synthesis of the *N*-aryl-*N'*-alkyl β -diketimine ligand sets.

presence of an equimolar amount of TsOH, to afford the desired *N*-aryl-*N'*-alkyl β -diketimine ligands (L^1H – L^4H ; Scheme 1) in 50–60% yield. The L^3H was synthesized recently by similar two-step procedure but no crystal structure was reported.^{10,19} These ligands were characterized by 1H NMR, $^{13}C\{^1H\}$ NMR and mass spectroscopy as well as elemental analysis. Crystal suitable for X-ray diffraction study of L^3H was obtained from hexane at -20 °C. Fig. 1 shows the expected planar conformation of an β -diketimine (NCCCN) backbone of L^3H with an almost perpendicular 2,6-diisopropylphenyl ring (the inter-planar angle between the phenyl ring and the NCCCN plane is 98.7°). The pyridylmethyl arm was found to swing away from the NCCCN backbone. According to the literature data on β -diketimine compounds,^{20–25} the bond length within NCCCN backbone can vary significantly. In the case of 2-amino-4-iminopent-2-enes, the bonding mode can be either delocalization (Δ_{C-C} , Δ_{C-N} <

0.01 Å)³⁴ or clear bond alternation ($\Delta_{C-C} = 0.08$ Å, $\Delta_{C-N} = 0.06$ Å).^{35,37} The obvious differences in the L^3H ($\Delta_{C-C} = 0.064$ Å, $\Delta_{C-N} = 0.045$ Å) showed the localized bond feature in the imine-enamine backbone.

Synthesis and structure characterization of asymmetrical β -diketiminato zinc complexes

The reactions of β -diketimine ligands L^1H – L^4H with diethyl zinc in a 1 : 1 molar ratio in *n*-hexane at -94 °C readily produced the corresponding zinc complexes [L^1ZnEt]₂ (1), [L^2ZnEt] (2), [L^3ZnEt]₂ (3), [L^4ZnEt] (4) (Scheme 2), with the elimination of ethane.

Single crystals of zinc complexes [L^1ZnEt]₂ (1), [L^2ZnEt] (2), [L^3ZnEt]₂ (3), and [L^4ZnEt] (4) suitable for X-ray diffraction characterization were obtained from saturated hexane solution at -20 °C. Selected bond lengths and angles are summarized in Table 1 for comparison. The crystallographic analysis results showed that complexes 1 and 3 are dinuclear, both consist of two β -diketiminato zinc subunits bridged by two pyridylmethyleneamide linkers forming a ten-membered metal-lamacrocycle (Fig. 2 and 3). Each Zn center assumes distorted tetrahedral coordination geometry. Only half of complex 1 or 3 is observed in the asymmetric unit which is related to other half by a crystallographic imposed C_2 symmetry. Report on crystal structure of complex 3 appeared during the preparation of the current manuscript.¹⁰ We kept the structural plot (Fig. 3) for the sake of easy comparison. For mononuclear complexes 2 and 4, the zinc centers assume distorted tetrahedral geometry coordinated by tridentate β -diketiminato ligand and an ethyl group (Fig. 4 and 5). The major structural difference between pair 1 & 3 and pair 2 & 4, other than the obvious different nuclearity, is their chain length of the pyridine arm on the β -diketiminato ligands. Complex 1 & 3 have shorter C_1 (one methylene) pyridine arm while complex 2 & 4 have longer C_2 (two methylenes) pyridine arm. From Table 1, one can see that both 2 & 4 bearing

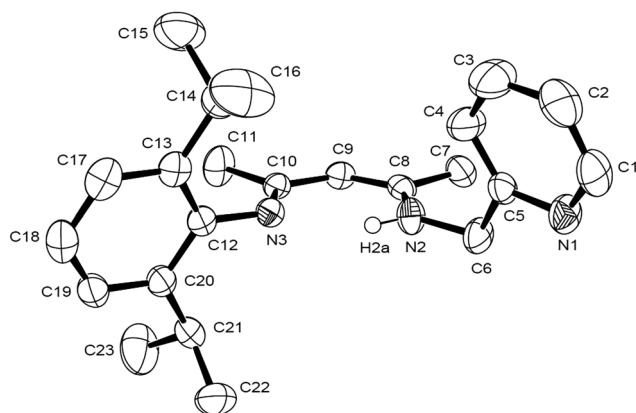
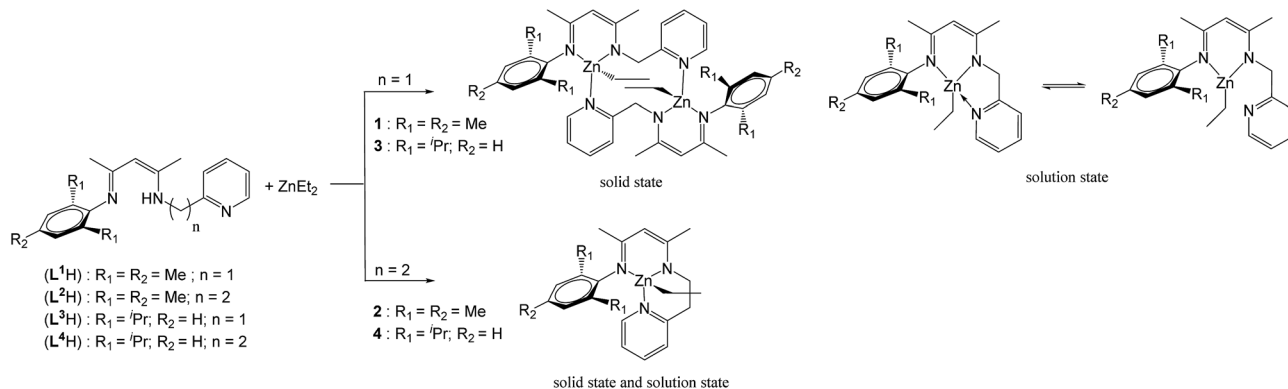


Fig. 1 ORTEP representation of the X-ray structure of L^3H at the 50% probability level. Hydrogen atoms were not shown for clarity. Selected bond lengths (Å): N(2)–C(8) 1.350(4), C(8)–C(9) 1.367(5), C(9)–C(10) 1.431(5), C(10)–N(3) 1.305(4).



Scheme 2 Synthesis procedure of the zinc complexes.

Table 1 Structural parameters of complexes 1, 2, 3, and 4^{ab}

	1	2	3	4
Zn–N _{aryl} ^a	2.012(6)	2.025(2)	2.0379(17)	2.023(2)
Zn–N _{alkyl}	2.009(6)	2.017(2)	2.0208(17)	2.012(2)
Zn–N _{py}	2.305(7)	2.174(2)	2.2672(18)	2.170(3)
Zn–C _{eth}	1.972(8)	2.003(3)	1.994(2)	1.995(3)
NCCN → Zn ^c	0.121	0.375	0.239	0.560
N _{aryl} –Zn–N _{alkyl} ^b	94.2(2)	93.61(10)	94.14(7)	93.34(9)
N _{aryl} –Zn–N _{py}	101.4(2)	114.36(10)	103.04(7)	109.91(10)
N _{alkyl} –Zn–N _{py}	88.8(2)	88.20(9)	90.58(7)	89.33(11)
N _{aryl} –Zn–C _{eth}	116.8(3)	119.85(12)	116.52(9)	125.72(12)
N _{alkyl} –Zn–C _{eth}	133.8(3)	133.79(12)	130.62(9)	123.49(12)
N _{py} –Zn–C _{eth}	115.2(3)	103.47(12)	116.20(9)	108.01(13)

^a Bond length are listed in Å. ^b Bond angles are given in degrees. ^c The distance between zinc atom and the NCCCN mean plane.

C₂ pyridine arm showed shorter Zn–N_{py} bond length compared with that of the C₁ arm bearing complexes (1 and 3). This means that the C₂ pyridine arm has a stronger coordination

bond with zinc center than the C₁ pyridine arm. This stronger Zn–N_{py} bond plus the ring strain of six-membered coordination ring in complexes 2 & 4 caused a higher out-of-plane (the NCCCN mean plane of β-diketiminato ligand) distance of the zinc atoms (Table 1, zinc out-of-plane distances: 0.375 & 0.560 Å for 2 & 4 vs. 0.121 & 0.239 Å for 1 & 3). All four zinc complexes were characterized by ¹H NMR, ¹³C{¹H} NMR and elemental analysis.

Solution behavior of asymmetrical β-diketiminato zinc complexes

In order to investigate if the solution structures of zinc complexes 1–4 are the same as their solid state structures, the diffusion-ordered spectroscopy (DOSY) technique was performed to gain insight into the behavior of these complexes in solution. DOSY is a powerful tool to obtain molecular parameters such as formula weight (FW) and hydrodynamic radii.^{26–30} Each time an NMR tube with toluene-*d*⁸ solvent was loaded with zinc complex and three internal references. Diffusion

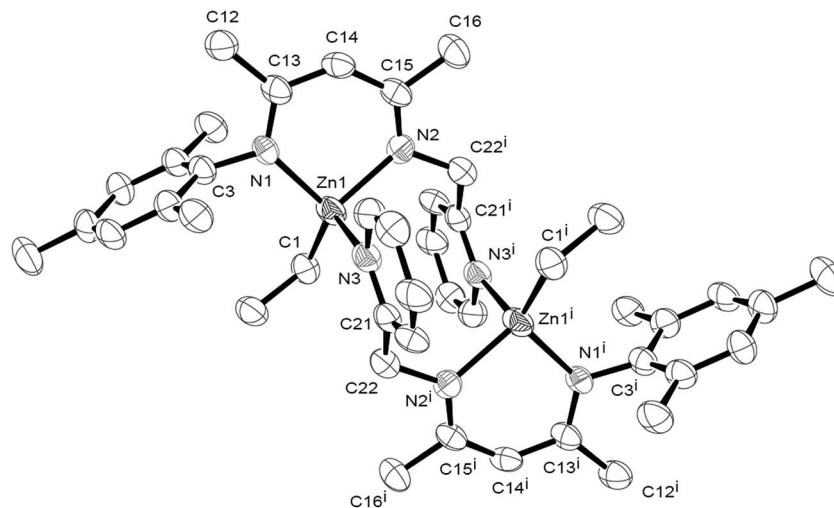


Fig. 2 ORTEP drawing of 1 [L^1ZnEt]₂ (non-hydrogen atoms) with ellipsoids drawn at the 50% probability level. Selected bond lengths (Å) and bond angles (deg): Zn(1)–N(1) 2.012(6), Zn(1)–N(2) 2.009(6), Zn(1)–N(3) 2.305(7), Zn(1)–C(1) 1.972(8), N(1)–Zn(1)–N(2) 94.2(12), N(1)–Zn(1)–N(3) 101.4(2), N(2)–Zn(1)–N(3) 88.8(2), N(1)–Zn(1)–C(1) 116.8(3), N(2)–Zn(1)–C(1) 133.8(3), and N(3)–Zn(1)–C(1) 115.2(3).

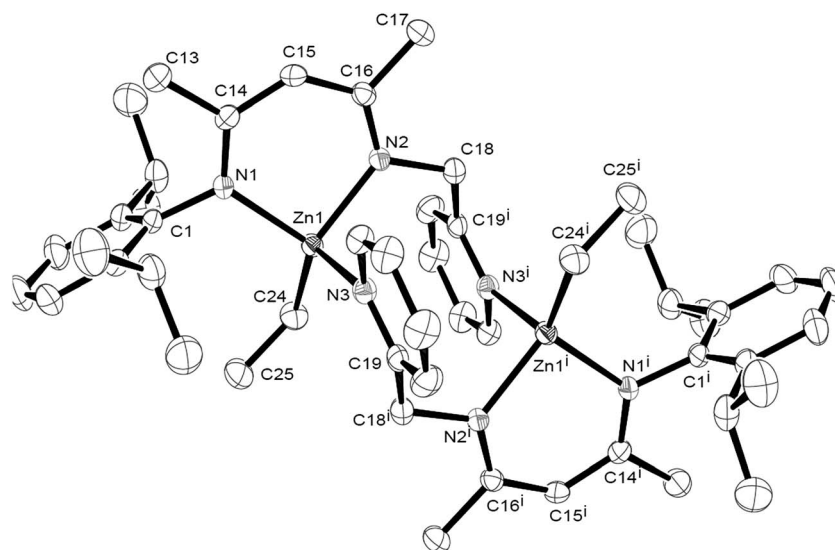


Fig. 3 ORTEP drawing of **3** [L^3ZnEt]₂ (non-hydrogen atoms) with ellipsoids drawn at the 50% probability level. Selected bond lengths (Å) and bond angles (deg): Zn(1)–N(1) 2.0379(17), Zn(1)–N(2) 2.0208(17), Zn(1)–N(3) 2.2672(18), Zn(1)–C(24) 1.994(2), N(1)–Zn(1)–N(2) 94.14(7), N(1)–Zn(1)–N(3) 103.04(7), N(1)–Zn(1)–N(2) 90.58(7), N(1)–Zn(1)–C(24) 116.52(9), N(2)–Zn(1)–C(24) 130.62(9), N(3)–Zn(1)–C(24) 116.20(9).

coefficient (D) and FW values of zinc complexes **1–4** are given in the ESI.† The diffusion coefficient of $1.15 \times 10^{-9} \text{ m}^2 \text{ s}^{-1}$ for **2** (FW of 425.09) and $1.06 \times 10^{-9} \text{ m}^2 \text{ s}^{-1}$ for **4** (FW of 457.78) are both in agreement with the monomeric form as seen from the X-ray studies (2.54% error for **2** and 2.33% error for **4**). On the other hand, the diffusion coefficients for **1** and **3** are $1.22 \times 10^{-9} \text{ m}^2 \text{ s}^{-1}$ (FW of 431.84; 7.71% error) and $0.82 \times 10^{-9} \text{ m}^2 \text{ s}^{-1}$ (FW of 501.17; 13.4% error), respectively. The DOSY experiments of **1** and **3** suggested that their solution state structure should be

mononuclear zinc complex instead of the dinuclear structure in solid state. The formation of the monomeric form in solution is possibly connected to more stable chelation binding mode than bridged dimerization binding mode in comparisons of the Zn–N_{py} distance of solid state (2.267 and 2.305 Å for dimeric complex **1** and **3**; 2.170 and 2.174 Å for monomeric complex **2** and **4**). Therefore, dimeric complexes **1** and **3** may be easier to dissociate their bridged pyridyl methylene arms than monomeric complexes **2** and **4**.

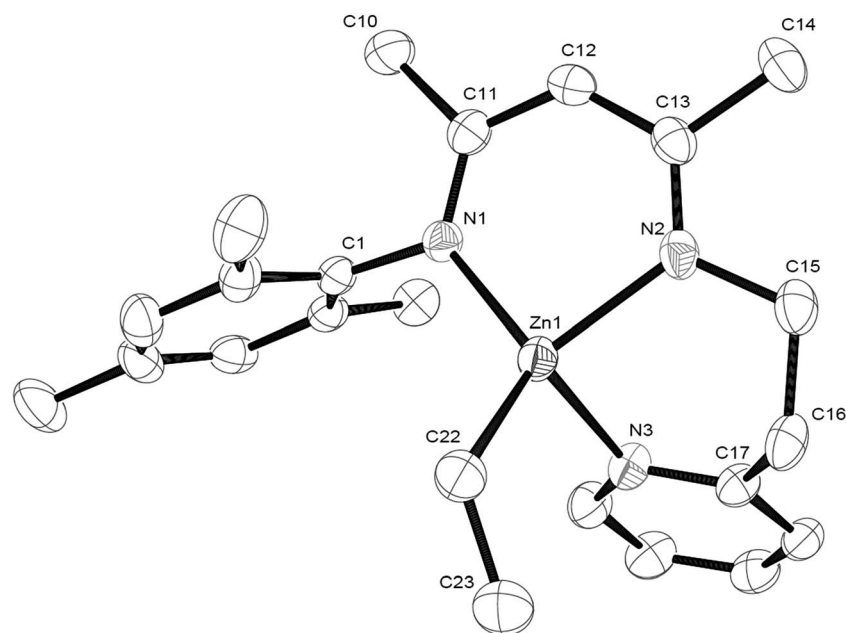


Fig. 4 ORTEP drawing of **2** [L^2ZnEt] (non-hydrogen atoms) with ellipsoids drawn at the 50% probability level. Selected bond lengths (Å) and bond angles (deg): Zn–N(1) 2.025(2), Zn–N(2) 2.017(2), Zn–N(3) 2.174(2), Zn–C(22) 2.003(3), N(1)–Zn(1)–N(2) 93.61(10), N(1)–Zn(1)–N(3) 114.36(10), N(2)–Zn(1)–N(3) 88.20(9), N(1)–Zn(1)–C(22) 119.85(12), N(2)–Zn(1)–C(22) 133.79(12), N(3)–Zn(1)–C(22) 103.47(12).

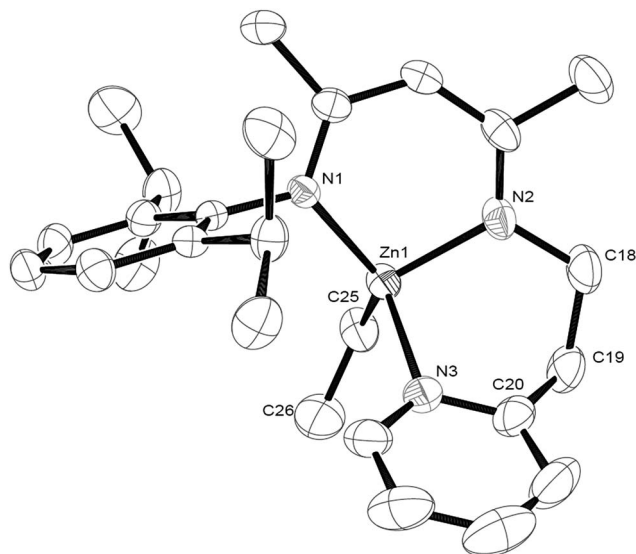


Fig. 5 ORTEP drawing of **4** [L^4ZnEt] (non-hydrogen atoms) with ellipsoids drawn at the 50% probability level. Selected bond lengths (Å) and bond angles (deg): Zn(1)–N(1) 2.023(2), Zn(1)–N(2) 2.012(2), Zn(1)–N(3) 2.170(3), Zn(1)–C(25) 1.995(3), N(1)–Zn(1)–N(2) 93.34(9), N(1)–Zn(1)–N(3) 109.91(10), N(2)–Zn(1)–N(3) 89.33(11), N(1)–Zn(1)–C(25) 125.72(12), N(2)–Zn(1)–C(25) 123.49(12), N(3)–Zn(1)–C(25) 108.01(13).

To further support the monomeric behavior of solution for all ethyl Zn complexes, the variable temperature 1H NMR (VT NMR) of complexes **1** and **2** were examined and shown in Fig. 6, S29 and S30.† The signal of the pyridine α -proton of complex **1** was obviously shifted from 8.02 ppm (at 293 K) to 7.59 ppm (at 183 K) while that of complex **2** was essentially unchanged (7.87 to 7.90 ppm). The VT NMR results were in accord with the

postulation that on-off coordination of the pyridine arm occurred in complex **1** but not in **2**. Similar case on the different chemical shifts of pyridine α -protons between pyridine dissociation and association in Zn complexes have been reported previously.^{31–33} Based on these observations, the C_1 pyridyl arm may be easier dissociation than the C_2 pyridyl arm, which is also consistent with crystallographic Zn– N_{py} distances shown above. More importantly, only one singlet is displayed for the methylene protons of the C_1 pyridyl arm of complexes **1** and **3**, while two triplets are displayed for the CH_2CH_2 of the C_2 pyridyl arm of complexes **2** and **4**, which however seem to be inconsistent with the coordination of pyridyl arm to the zinc metal center. A stable coordination of pyridyl arm to zinc center would cause the two methylene protons of C_1 pyridyl arm to be diastereotopic, therefore displayed as two doublets; a similar situation will occur for the CH_2CH_2 of the C_2 pyridyl arm, with more complicated coupling modes being expected. Another possibility for the monomeric pyridyl arm chelating complex **2** may undergo a six-member ring fluxional mechanism to cause the broadening signals of CH_2CH_2 in the C_2 pyridyl arm region. Talking all these into consideration, probably some dynamic processes involving reversible dissociation and association of the C_1 pyridyl arm in the complexes **1** and **3** may take place in solution at ambient temperature. In fact, in the VT NMR spectra, broadening of these signals are observed at low temperatures, with that of complex **1** more significant, suggesting a stable coordination state will be reached soon. The C_2 pyridyl arm complexes **2** and **4** remain them chelating mode in the solution due to the unchanged pyridine α -protons in VT NMR. Therefore, based on the above discussions we assume the possible solution conformations for complexes **1–4** in Scheme 2 and Fig. 6.

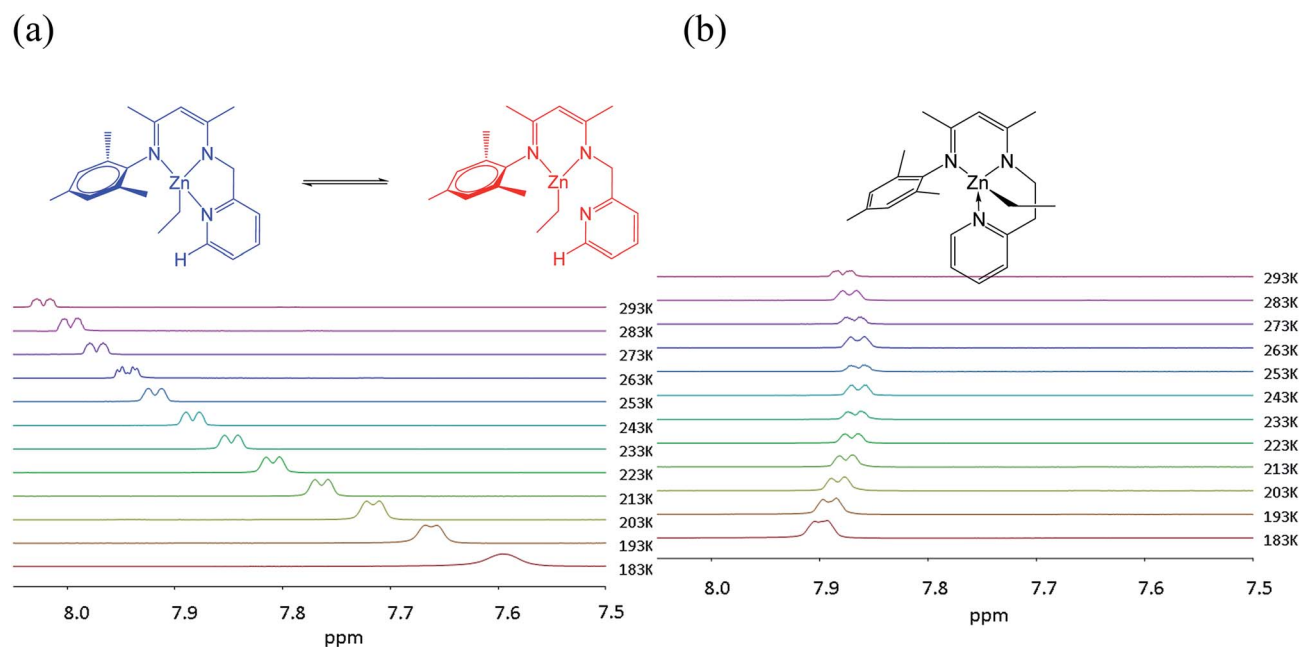


Fig. 6 Variable temperature 1H NMR experiment of the pyridine α -proton of complexes **1** and **2** (7.50–8.05 ppm).

Ring-opening polymerization of L-lactide

Complexes 1–4 were used as the catalysts with benzyl alcohol (BnOH) as a initiator for the ring-opening polymerization of L-lactide in CH₂Cl₂ at room temperature. The polymerization results are listed in Table 2, in which complex 1 was the most active catalyst for the polymerization of L-lactide producing polymers with narrow polydispersity index (PDI). The observed $M_{n(\text{GPC})}$ values (entries 1–4, Table 2) were smaller than the calculated M_n values, which were similar to the $M_{n(\text{NMR})}$ (Fig. 7). This implies that intra-molecular transesterification occurred even though the $M_{n(\text{GPC})}$ value slightly increased with an increase in the ratio of [LA]₀/[BnOH]. Other catalysts displayed similar effects. In addition, complex 1 revealed higher catalytic activity than Zn complex bearing NNO-tridentate β-diketiminato ([LA]₀/[Zn] = 100 : 1, in CH₂Cl₂, at ambient temperature, 40 min, conversion = 83%).¹⁰ It implied that benzyl alkoxide is the better initiator than phenolate.

Table 2 clearly indicated a decreasing order of catalytic activity from complexes 1 to 4 (1 > 2 >> 3 > 4). This indicates that the most influencing factor of the reactivity is the steric repelling feature on the substituents of phenyl groups. The bulky isopropyl substituents on phenyl groups in 3 and 4 are a disadvantage to catalytic activity. We believe the introduction of steric bulky groups to the phenyl rings decreases the space around the zinc center and blocks the coordination between LA and zinc center. In addition, the short-arm complexes 1 and 3 showed the greater catalytic activity than their long-arm analogues 2 and 4, due to the instability of shorter chelating ring. Indeed, crystallographic data revealed that zinc complexes with the pyridin-2-ylethyl group (2 & 4) tend to form six-membered ring mononuclear form while a ten-membered ring dimeric structure was obtained with ligands of pyridin-2-ylmethyl group (1 & 3). According to DOSY studies of all four zinc complexes, however, they are all mononuclear in solution. It was also reported in the literature¹⁰ that the dimeric ethyl Zn analogue bearing the same β-diketiminato ligands with pyridin-2-ylmethyl group (C₁ pyridyl arm) reacted with phenol and became monomeric Zn phenolate complexes. This further indicates that five-membered-ring zinc complexes 1 and 3 with pyridin-2-ylmethyl group may be easier to dissociate than zinc

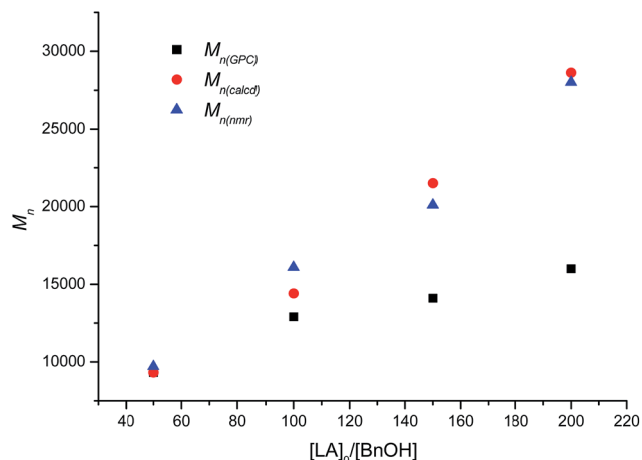


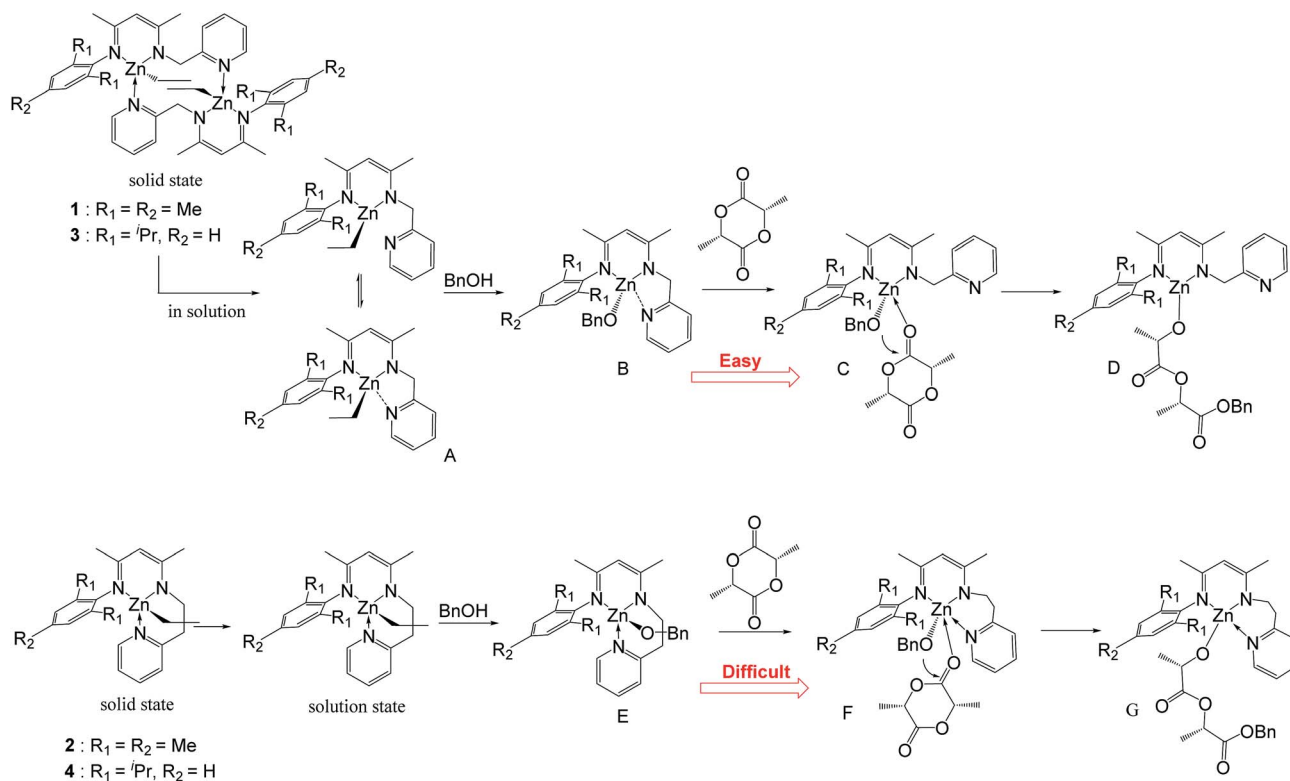
Fig. 7 Linear plot of $M_{n(\text{GPC})}$, $M_{n(\text{NMR})}$, and $M_{n(\text{calcd})}$ vs. $[\text{LA}]_0 \times \text{conv.} / [\text{BnOH}]$ (red circles are $M_{n(\text{calcd})}$, blue triangles are $M_{n(\text{NMR})}$, and black squares are $M_{n(\text{GPC})}$).

complexes 2 and 4. Therefore we postulate that during the polymerization process, zinc complexes 1 and 3 reacted with BnOH to form monomeric benzyl alkoxide Zn complexes also (B in Scheme 3). Since in the monomeric form the shorter C₁ pyridyl arm in β-diketiminato ligand forms five-membered chelate ring while the longer C₂ pyridyl arm forms the six-membered ring, it is easy to understand the shorter arm complexes (1 & 3) have higher tendency to open up the more strained five-membered ring than the longer-arm complexes (2 & 4). Because of the easier dissociation of pyridin-2-ylmethyl arm in complexes 1 and 3, it is easy for the coordination of L-lactide with zinc atom to form C in Scheme 3. Following the initiation of benzyl alkoxide to L-lactides, three-coordinate zinc complex (D in Scheme 3) was formed with dangling pyridin-2-ylmethyl arm due to the open-up of the unstable five-membered-ring. As for complexes 2 and 4, they initially also transformed into benzyl alkoxide zinc complexes E in Scheme 3 after reacting with BnOH. However the following step is different. Since the six-membered ring zinc complexes with pyridin-2-ylethyl arm are stable, it is reluctant to open up. Therefore, upon L-lactide coordination, a 5-coordinate zinc

Table 2 With L-LA polymerization initiated by complexes 1–4 at room temperature

Entry	Complex	<i>T</i> (min)	Conv. ^c (%)	$M_{n(\text{GPC})}$ ^a	$M_{n(\text{calcd})}$ ^b	$M_{n(\text{NMR})}$ ^c	PDI ^a	k_{obs} ^d (s ⁻¹)
1	1	15	>99	12 900	14 400	16 100	1.06	0.299
2 ^e	1	15	>99	9300	7200	9700	1.04	—
3 ^f	1	15	>99	14 100	21 500	20 100	1.01	—
4 ^g	1	15	>99	16 000	28 600	28 000	1.01	—
5	2	50	>99	11 900	14 400	11 700	1.01	0.100
6	3	360	93	12 600	13 500	8300	1.01	0.006
7	4	360	89	11 700	6500	9200	1.02	0.005

^a Obtained from GPC analysis and calibrated according to polystyrene standards. ^b Calculated from the molecular weight of L-lactide $\times [\text{M}]_0 / [\text{BnOH}]_0 \times \text{conversion yield plus } M_w(\text{BnOH})$. ^c Obtained from ¹H NMR analysis. ^d $[\text{LA}]_0 / [\text{Zn} + \text{BnOH}] = 100$; $[\text{LA}]_0 = 1.00 \text{ M}$ in CH₂Cl₂ for 1–3 or $[\text{LA}]_0 / [\text{Zn} + \text{BnOH}] = 50$; $[\text{LA}]_0 = 1.32 \text{ M}$ in CDCl₃ for 4. ^e $[\text{LA}]_0 / [\text{cat.}] / [\text{BnOH}]$ ratio was 50 : 0.5 : 1. ^f $[\text{LA}]_0 / [\text{cat.}] / [\text{BnOH}]$ ratio was 150 : 0.5 : 1. ^g $[\text{LA}]_0 / [\text{cat.}] / [\text{BnOH}]$ ratio was 200 : 0.5 : 1.



Scheme 3 Differences between dimeric and monomeric Zn complexes during the L-lactide polymerization.

complex (F in Scheme 3) could be formed. Following the attack of benzyl alkoxide to L-lactides, a four-coordinate zinc complex (G in Scheme 3) could be formed keeping the coordination of pyridin-2-ylethyl arm intact. Because the six-membered ring was stabilized by the intra-chelation of the pyridin-2-ylethyl arm, there was less space around zinc center for G than the three-coordinate D. This decreased the efficacy of L-lactide coordination in G provide a good rationale for the lower catalytic activity for 2 and 4.

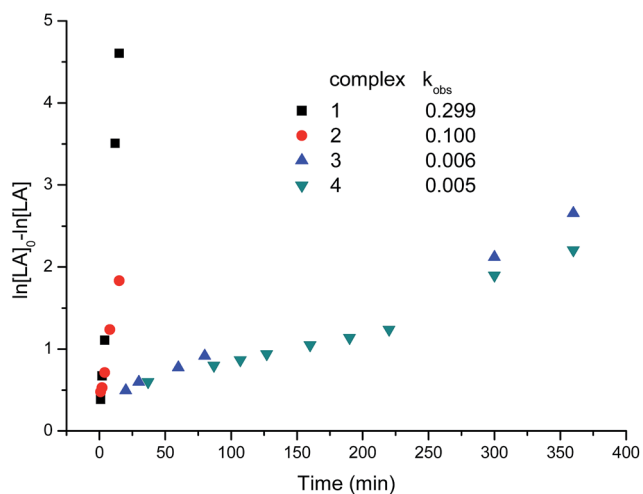


Fig. 8 First-order kinetic plots for L-LA polymerizations with time with 1–4.

Kinetic study of the polymerization of L-lactide by 1–4

A kinetic study was performed in order to determine the reaction order of L-lactide in the polymerization of L-lactide with zinc complexes and BnOH. Conversion of L-lactide over time was recorded by ¹H NMR for zinc complexes and BnOH of various concentrations at 25 °C until L-lactide consumption was completed ($[LA]_0/[Zn + BnOH] = 100$; $[LA]_0 = 1.00$ M in CH₂Cl₂ for 1–3 or $[LA]_0/[Zn + BnOH] = 50$; $[LA]_0 = 1.32$ M in CDCl₃ for 4). Plots of $\ln([LA]_0/[LA])$ vs. time in a wide range of $[LA]_0$ are linear, showing that polymerization proceeds with a first-order dependence on [L-lactide] (Fig. 8, $k_{\text{obs}} = 0.299$ s⁻¹ for 1, 0.100 s⁻¹ for 2, 0.006 s⁻¹ for 3, and 0.005 s⁻¹ for 4). Therefore the rate of polymerization can be described as $-d[LA]/dt = k_{\text{obs}}[LA]$. The kinetic data showed that the steric effect increased the catalytic activity by more than 50 folds and the chelating effect increased the catalytic activity by more than 2 fold.

Conclusions

Zinc complexes 1–4 supported by asymmetrical β-diketiminato ligands were readily synthesized. The dimeric 1, 3 and monomeric 2, 4 were elucidated by X-ray diffraction techniques. Diffusion-ordered NMR spectroscopy (DOSY) experiments, however, have shown that all zinc complexes are mononuclear in solution state. The effect of the ligand structure on the ROP of L-lactide proved to be significant. It was found that steric bulky substituents hindered L-lactide coordination to Zn and hence decreased the catalytic activity of the corresponding Zn

complex. The ligands with the longer pyridin-2-ylethyl arm can form a stable six-membered ring by the arm and lessen the chance for L-lactide coordination. Conversely, the ligands with the shorter pyridin-2-ylmethyl arm form mononuclear zinc complexes in solution state that is prone to dissociation. Freeing the coordination site causes higher chance for L-lactide coordination and thus increases the catalytic activity for the shorter arm complexes.

Experimental section

All manipulations were carried out under an atmosphere of purified dinitrogen in the dry box, or using standard Schlenk techniques. Chemical reagents were purchased from Aldrich Chemical Co. Ltd., Lancaster Chemicals Ltd., or Fluka Ltd. All the reagents were used without further purification, apart from all solvents that were dried over Na (Et₂O, THF) or CaH₂ (CH₂Cl₂, CH₃CN) and then thoroughly degassed before use. 2-((2,6-Diisopropylphenyl)imido)-2-penten-4-one³⁴ and 2-((2,4,6-trimethylphenyl)imido)-2-penten-4-one³⁵ were synthesized by following the published procedure. ¹H and ¹³C{¹H} NMR spectra were recorded using a Varian Gemini-200 or Varian Unity Plus-400 FT-NMR spectrometer. Proton and carbon shifts are relative to internal Me₄Si or solvent resonance. ESI mass spectra were collected on a Waters ZQ 4000 mass spectrometer. Microanalysis was performed using a Heraeus CHN-O-RAPID instrument. GPC measurements were performed on a Jasco PU-2080 PLUS HPLC pump system equipped with a differential Jasco RI-2031 PLUS refractive index detector using THF (HPLC grade) as an eluent (flow rate 1.0 mL min⁻¹, at 40 °C). The chromatographic column was JORDI Gel DVB 103 Å, and the calibration curve was made according to primary polystyrene standards to calculation of M_n(GPC).

Ligand synthesis

The synthesis of L¹H–L⁴H were carried out using similar procedures. As a representative example the synthesis of L¹H is given below in detail.

L¹H. The reaction of 2-((2,4,6-trimethylphenyl)imido)-2-penten-4-one (8.38 g, 38.6 mmol), 2-(aminomethyl)pyridine (4.17 g, 38.6 mmol), and *p*-toluenesulfonic acid (7.34 g, 38.6 mmol) were dissolved in toluene (60 mL) and refluxed for 18 h using a Dean–Stark apparatus to collect water. The volatiles were removed under vacuum to give a yellow solid that was extracted with dichloromethane (100 mL) and the resultant solution was stirred for 1 h with a saturated solution of sodium carbonate (100 mL). The organic layer was separated, dried over MgSO₄, and concentrated to give crude product. Recrystallization of the crude product from hexane gave pure L¹H as a yellow solid (6.68 g, 56% yield). ¹H NMR (C₆D₆, 400 MHz, 298 K): δ 11.44 (bs, 1H, NH), 8.39 (ddd, 1H, *J* = 4.8 Hz, 1.8 Hz, 1.0 Hz, Py-*H_α*), 7.10–6.55 (m, 6H, Ar-*H* and Py-*H*), 4.73 (s, 1H, backbone-CH), 4.32 (s, 2H, CH₂Py), 2.25 (s, 3H, *para* PhCH₃), 2.20 (s, 6H, *ortho* PhCH₃), 1.65 (s, 3H, backbone-CH₃), 1.64 (s, 3H, backbone-CH₃). ¹³C{¹H} NMR (C₆D₆, 100.06 MHz, 298 K): δ 167.38, 161.48, 156.22, 150.20, 148.30, 136.92, 131.88, 129.75, 128.26,

122.30, 120.97, 95.71, 49.67, 21.89, 21.62, 19.72, 19.29. Anal. calcd for C₂₀H₂₅N₃: C, 78.14; H, 8.20; N, 13.67. Found: C, 78.20; H, 8.16; N, 13.61. ESI-MS *m/z* = 308.23 ([M + H]⁺).

L²H. The reaction of 2-((2,4,6-trimethylphenyl)imido)-2-penten-4-one (2.10 g, 9.65 mmol), 2-(aminoethyl)pyridine (1.18 g, 9.65 mmol), and *p*-toluenesulfonic acid (1.84 g, 9.65 mmol) were carried out following a procedure similar to L¹H synthesis. Yield: 2.02 g (66%). ¹H NMR (C₆D₆, 400 MHz, 298 K): δ 11.08 (bs, 1H, NH), 8.40 (d, 1H, *J* = 4.9 Hz, 1.8 Hz, 1.0 Hz, Py-*H_α*), 6.92–6.54 (m, 6H, Ar-*H* and Py-*H*), 4.63 (s, 1H, backbone-CH), 3.44 (t, 2H, *J* = 3.6 Hz, CH₂CH₂Py), 2.75 (t, 2H, *J* = 6.4 Hz, CH₂CH₂Py), 2.27 (s, 3H, *para* PhCH₃), 2.10 (s, 6H, *ortho* PhCH₃), 1.62 (s, 3H, backbone-CH₃), 1.60 (s, 3H, backbone-CH₃). ¹³C{¹H} NMR (C₆D₆, 100.06 MHz, 298 K): δ 166.79, 160.15, 156.07, 150.43, 148.39, 136.39, 131.55, 129.50, 128.37, 124.30, 121.90, 94.41, 43.66, 40.23, 21.80, 21.66, 19.75, 19.29. Anal. calcd for C₂₁H₂₇N₃: C, 78.46; H, 8.47; N, 13.07. Found: C, 78.49; H, 8.50; N, 13.06. ESI-MS *m/z* = 322.25 ([M + H]⁺).

L³H. 2-(2,6-Diisopropylphenylimido)-2-pentene-4-one (10 g, 38.6 mmol), 2-(aminomethyl)pyridine (4.17 g, 38.6 mmol), and *p*-toluenesulfonic acid (7.34 g, 38.6 mmol) were carried out following a procedure similar to L¹H synthesis. Recrystallization of the crude product from hexane gave pure L³H as a yellow solid (7.35 g, 55% yield). ¹H NMR (C₆D₆, 400 MHz, 298 K): δ 11.52 (bs, 1H, NH), 8.38 (ddd, 1H, *J* = 4.5 Hz, 2.0 Hz, 1.2 Hz, Py-*H_α*), 7.07–6.56 (m, 6H, Ar-*H* and Py-*H*), 4.74 (s, 1H, backbone-CH), 4.36 (s, 2H, CH₂Py), 3.17 (septet, 2H, *J* = 7 Hz, ArCH(CH₃)₂), 1.68 (s, 3H, backbone-CH₃), 1.66 (s, 3H, backbone-CH₃), 1.23 (d, 6H, *J* = 7 Hz, ArCH(CH₃)₂), 1.18 (d, 6H, *J* = 7 Hz, ArCH(CH₃)₂). ¹³C{¹H} NMR (C₆D₆, 100.06 MHz, 298 K): δ 167.17, 160.76, 156.03, 149.98, 147.68, 138.58, 136.63, 123.85, 123.63, 122.11, 120.73, 95.35, 49.42, 28.92, 24.50, 23.51, 22.13, 19.46. Anal. calcd for C₂₃H₃₁N₃: C, 79.04; H, 8.94; N, 12.02. Found: C, 79.00; H, 8.97; N, 11.95. ESI-MS *m/z* = 350.41 ([M + H]⁺).

L⁴H. The reaction of 2-(2,6-diisopropylphenylimido)-2-pentene-4-one (2.65 g, 10.3 mmol), 2-(aminoethyl)pyridine (1.26 g, 10.3 mmol), and *p*-toluenesulfonic acid (1.96 g, 10.3 mmol) were carried out following a procedure similar to L¹H synthesis. Yield: 2.13 g (57%). ¹H NMR (C₆D₆, 400 MHz, 298 K): δ 11.14 (bs, 1H, NH), 8.39 (ddd, 1H, *J* = 4.0 Hz, 1.9 Hz, 1.0 Hz, Py-*H_α*), 7.13–6.56 (m, 6H, Ar-*H* and Py-*H*), 4.64 (s, 1H, backbone-CH), 3.49 (t, 2H, *J* = 7 Hz, CH₂CH₂Py), 3.11 (septet, 2H, *J* = 7 Hz, ArCH(CH₃)₂), 2.83 (t, 2H, *J* = 7 Hz, CH₂CH₂Py), 1.65 (s, 3H, backbone-CH₃), 1.63 (s, 3H, backbone-CH₃), 1.22 (d, 6H, *J* = 7 Hz, ArCH(CH₃)₂), 1.20 (d, 6H, *J* = 7 Hz, ArCH(CH₃)₂). ¹³C{¹H} NMR (C₆D₆, 100.06 MHz, 298 K): δ 166.75, 159.75, 155.88, 150.64, 147.93, 138.59, 136.16, 123.72, 123.62, 123.56, 123.68, 94.22, 43.33, 40.24, 28.86, 24.50, 23.52, 22.10, 19.51. Anal. calcd for C₂₄H₃₃N₃: C, 79.29; H, 9.15; N, 11.56. Found: C, 79.22; H, 9.16; N, 11.51. ESI-MS *m/z* = 364.12 ([M + H]⁺).

Zinc complexes synthesis

[L¹ZnEt]₂ (**1**). In an inert atmosphere a solution of diethylzinc solution (3.26 mmol) was added dropwise into the L¹H (1.0 g, 3.26 mmol) solution in 3 mL of hexane at –94 °C. The color changed from yellow to red during warm-up. After stirring

at room temperature for 12 h, the solvent was removed under vacuum and the residue extracted with 75 mL of hexane and filtered through a plug of Celite. The volume was reduced and the solution was placed at $-20\text{ }^{\circ}\text{C}$ overnight, yielding red crystalline solids (1.18 g, 90%). ^1H NMR (C_6D_6 , 200 MHz, 298 K): δ 8.02 (d, $J = 5.3$ Hz, 1H, Py1), δ 6.94 (s, 2H, Ph), δ 6.85 (td, $J = 7.6$ Hz, 1H, Py3), δ 6.47 (d, $J = 7.9$ Hz, 1H, Py4), δ 6.41 (d, $J = 6.6$ Hz, 1H, Py2), δ 4.81 (s, 1H, $\text{CH}(\text{C}=\text{N})_2$), δ 4.47 (s, 2H, CH_2Py), δ 2.29 (s, 6H, *ortho* PhCH_3), δ 2.23 (s, 3H, *para* PhCH_3), δ 1.80 (s, 3H, $\text{CH}_3(\text{C}=\text{N})$), δ 1.71 (s, 3H, $\text{CH}_3(\text{C}=\text{N})$), δ 1.25 (t, $J = 8.1$ Hz, 3H, ZnCH_2CH_3), δ 0.44 (q, $J = 8.1$ Hz, 2H, ZnCH_2CH_3). ^{13}C NMR (C_6D_6 , 101 MHz, 298 K) δ 165.54, 164.71, 159.30, 148.30, 147.09, 136.79, 132.83, 131.55, 129.25, 122.05, 121.70, 94.69, 54.42, 22.64, 21.94, 21.05, 18.85, 13.71, -0.90 . Anal. calcd for $\text{C}_{44}\text{H}_{58}\text{N}_6\text{Zn}_2$: C, 65.92; H, 7.29; N, 10.48. Found: C, 65.84; H, 7.25; N, 10.32.

[L^2ZnEt] (2). Following the procedure described for **1**, reaction of diethylzinc (3.26 mmol) and L^2H (1.05 g, 3.26 mmol) gave **2** as orange crystalline solids (1.29 g, 96%). ^1H NMR (C_6D_6 , 400 MHz, 298 K): δ 7.94 (ddd, $J = 5.1, 1.8, 0.9$ Hz, 1H, Py1), δ 6.95 (s, 2H, Ph), δ 6.83 (td, $J = 7.7, 1.8$ Hz, 1H, Py3), δ 6.45 (d, $J = 7.7$ Hz, 1H, Py4), δ 6.36 (ddd, $J = 7.6, 5.1, 1.2$ Hz, 1H, Py2), δ 4.70 (s, 1H, $\text{CH}(\text{C}=\text{N})_2$), δ 3.38 (t, $J = 6.9, 5.0$ Hz, 2H, $\text{CH}_2\text{CH}_2\text{Py}$), δ 2.77 (t, $J = 6.9, 5.0$ Hz, 2H, $\text{CH}_2\text{CH}_2\text{Py}$), δ 2.26 (s, 6H, *ortho* PhCH_3), δ 2.25 (s, 3H, *para* PhCH_3), δ 1.72 (s, 3H, $\text{CH}_3(\text{C}=\text{N})$), δ 1.67 (s, 3H, $\text{CH}_3(\text{C}=\text{N})$), δ 1.49 (t, $J = 8.1$ Hz, 3H, ZnCH_2CH_3), δ 0.62 (q, $J = 8.1$ Hz, 2H, ZnCH_2CH_3). ^{13}C NMR (C_6D_6 , 101 MHz, 298 K) δ 166.70, 164.36, 160.64, 148.39, 147.40, 137.23, 132.63, 132.05, 129.30, 124.43, 121.41, 94.29, 49.05, 37.19, 22.78, 21.54, 21.09, 18.86, 14.03, 1.28. Anal. calcd for $\text{C}_{23}\text{H}_{31}\text{N}_3\text{Zn}$: C, 66.58; H, 7.53; N, 10.13. Found: C, 65.54; H, 7.55; N, 10.10.

[L^3ZnEt]₂ (3). Following the procedure described for **1**, reaction of diethylzinc (2.86 mmol) and L^3H (1.0 g, 2.86 mmol) gave **3** as orange crystalline solids (1.11 g, 88%). ^1H NMR (C_6D_6 , 200 MHz, 298 K): δ 8.27 (d, 1H, $J = 4.7$, Py1), δ 7.19 (d, 3H, $J = 0.5$, Ph), δ 6.94 (td, 1H, $J = 7.8, 6.1$, Py3), δ 6.60 (d, 1H, $J = 7.6$, Py4), δ 6.51 (m, Py2), δ 4.84 (s, 1H, $\text{CH}(\text{C}=\text{N})_2$), δ 4.55 (s, 2H, CH_2Py), δ 3.41 (hept, 2H, $J = 7.3$, $\text{PhCH}(\text{CH}_3)_2$), δ 1.80 (s, 3H, $\text{CH}_3(\text{C}=\text{N})$), δ 1.74 (s, 3H, $\text{CH}_3(\text{C}=\text{N})$), δ 1.33 (d, 6H, $J = 6.8$, $\text{PhCH}(\text{CH}_3)_2$), δ 1.17–1.12 (m, 9H, $\text{PhCH}(\text{CH}_3)_2 + \text{ZnCH}_2\text{CH}_3$), δ 0.37 (q, 2H, $J = 8.1$, ZnCH_2CH_3). ^{13}C NMR (C_6D_6 , 101 MHz, 298 K): δ 166.44, 165.91, 159.68, 148.84, 146.33, 142.20, 136.53, 125.37, 123.72, 121.90, 121.54, 95.32, 54.90, 28.25, 24.65, 24.02, 23.57, 22.08, 13.26, -0.71 . Anal. calcd for $\text{C}_{50}\text{H}_{70}\text{N}_6\text{Zn}_2$: C, 67.83; H, 7.98; N, 9.39. Found: C, 67.79; H, 7.96; N, 9.49.

[L^4ZnEt] (4). Following the procedure described for **1**, reaction of diethylzinc (2.96 mmol) and L^4H (1.03 g, 2.96 mmol) gave **4** as orange crystalline solids (1.24 g, 92%). ^1H NMR (C_6D_6 , 200 MHz, 298 K): δ 8.23 (d, 1H, $J = 4.0$, Py1), δ 7.16 (s, 3H, Ph), δ 6.94 (t, 1H, $J = 7.6$, Py3), δ 6.62 (d, 1H, $J = 7.6$, Py4), δ 6.55–6.44 (m, 1H, Py2), δ 4.73 (s, 1H, $\text{CH}(\text{C}=\text{N})_2$), δ 3.67 (t, 2H, $J = 6.7$, $\text{CH}_2\text{CH}_2\text{Py}$), δ 3.31 (hept, 2H, $J = 6$, $\text{PhCH}_2(\text{CH}_3)_2$), δ 2.89 (t, 2H, $J = 6.6$, $\text{CH}_2\text{CH}_2\text{Py}$), δ 1.77 (s, 3H, $\text{CH}_3(\text{C}=\text{N})$), δ 1.69 (s, 3H, $\text{CH}_3(\text{C}=\text{N})$), δ 1.35 (t, 3H, $J = 8.0$, ZnCH_2CH_3), δ 1.20 (dd, 12H, $J = 9.9, 6.9$, $\text{PhCH}(\text{CH}_3)_2$), δ 0.51 (q, 2H, $J = 8.0$, ZnCH_2CH_3). ^{13}C NMR (C_6D_6 , 101 MHz, 298 K): δ 167.18, 165.69, 160.37, 149.35, 146.33, 142.34, 136.42, 125.31, 123.81, 123.76, 121.41, 95.55,

50.46, 39.74, 28.18, 24.46, 24.14, 23.56, 21.64, 13.37, -0.23 . Anal. calcd for $\text{C}_{26}\text{H}_{37}\text{N}_3\text{Zn}$: C, 68.34; H, 8.16; N, 9.20. Found: C, 68.39; H, 8.06; N, 9.15.

Typical polymerization procedure

A typical polymerization procedure was exemplified by the synthesis of PLA (entry 1, Table 2) at room temperature. The conversion yield (>99%) of PLA was analyzed by ^1H NMR spectroscopic studies. A mixture of the catalyst (0.1 mmol) and *L*-lactide (1.44 g, 10.0 mmol) in CH_2Cl_2 (10.0 mL) was stirred at room temperature for 15 min. Volatile materials were removed under vacuum, and the residue was redissolved in THF (5.0 mL). The mixture was then quenched through the addition of EtOH, and the polymer was precipitated by pouring it into *n*-hexane (80.0 mL) to yield white crystalline solids. Yield: 1.34 g (93%).

Kinetic study of polymerization of *L*-LA by **1**

L-LA (10.0 mmol) was added to a solution of **1** (0.1 mmol) and BnOH (0.1 mmol) in CH_2Cl_2 (10 mL). The mixture was then stirred at room temperature under N_2 . At appropriate time intervals, 0.2 mL aliquots were removed and then dried to a constant weight under vacuum and analyzed by ^1H NMR.

X-ray crystal structure determinations

All single-crystal X-ray diffraction data were measured on a Bruker Nonius Kappa CCD diffractometer using Mo K_α radiation ($\lambda = 0.71073\text{ \AA}$). The data collection was executed using the SMART program.³⁶ Cell refinement and data reduction were made with the SAINT program.³⁷ The structure was determined using the SHELXTL/PC program³⁸ and refined using full-matrix least-squares. All non-hydrogen atoms were refined anisotropically, whereas hydrogen atoms were placed at the calculated positions and included in the final stage of refinements with fixed parameters. Further details are given in Tables S1 and S2.†

Acknowledgements

Financial support of the Ministry of Science and Technology of Taiwan (102-2113-M-037-008-MY3, 104-2113-M-037-010) and NSYSU-KMU Joint Research Project (NSYSUKMU103-I004, NSYSUKMU 104-P006) are highly appreciated. We thank Mr Ting-Shen Kuo, National Taiwan Normal University for X-ray structural determinations and Mr Min-Yuan Hung, Center for Research Resources and Development of KMU for their facilities.

References

- (a) R. C. Jeske, A. M. DiCiccio and G. W. Coates, *J. Am. Chem. Soc.*, 2007, **129**, 11330–11331; (b) C. Robert, F. de Montigny and C. M. Thomas, *Nat. Commun.*, 2011, **2**, 586–592.
- (a) M. J. Stanford and A. P. Dove, *Chem. Soc. Rev.*, 2010, **39**, 486–494; (b) C. M. Thomas, *Chem. Soc. Rev.*, 2010, **39**, 165–173.
- C.-S. Ha and J. A. Gardella, *Chem. Rev.*, 2005, **105**, 4205–4232.

- 4 (a) A. P. Dove, V. C. Gibson, E. L. Marshall, A. J. P. White and D. J. Williams, *Dalton Trans.*, 2004, 570–578; (b) M. Cheng, A. B. Attygalle, E. B. Lobkovsky and G. W. Coates, *J. Am. Chem. Soc.*, 1999, **121**, 11583–11584; (c) B. M. Chamberlain, M. Cheng, D. R. Moore, T. M. Ovitt, E. B. Lobkovsky and G. W. Coates, *J. Am. Chem. Soc.*, 2001, **123**, 3229–3238.
- 5 K. Yu and C. W. Jones, *J. Catal.*, 2004, **222**, 558–564.
- 6 H.-Y. Chen, B.-H. Huang and C.-C. Lin, *Macromolecules*, 2005, **38**, 5400–5405.
- 7 H.-Y. Chen, Y.-L. Peng, T.-H. Huang, A. K. Sutar, S. A. Miller and C.-C. Lin, *J. Mol. Catal. A: Chem.*, 2011, **339**, 61–71.
- 8 F. d. r. Drouin, P. O. Oguadinma, T. J. J. Whitehorne, R. E. Prud'homme and F. Schaper, *Organometallics*, 2010, **29**, 2139–2147.
- 9 X. Xu, Y. Chen, G. Zou, Z. Ma and G. Li, *J. Organomet. Chem.*, 2010, **695**, 1155–1162.
- 10 Z. Dai, J. Zhang, Y. Gao, N. Tang, Y. Huang and J. Wu, *Catal. Sci. Technol.*, 2013, **3**, 3268–3277.
- 11 Z. Liu, W. Gao, J. Zhang, D. Cui, Q. Wu and Y. Mu, *Organometallics*, 2010, **29**, 5783–5790.
- 12 A. Otero, J. Fernández-Baeza, L. F. Sánchez-Barba, J. Tejada, M. Honrado, A. Garcés, A. Lara-Sánchez and A. M. Rodríguez, *Organometallics*, 2012, **31**, 4191–4202.
- 13 H.-Y. Chen, H.-Y. Tang and C.-C. Lin, *Macromolecules*, 2006, **39**, 3745–3752.
- 14 C.-H. Wang, C.-Y. Li, B.-H. Huang, C.-C. Lin and B.-T. Ko, *Dalton Trans.*, 2013, **42**, 10875–10884.
- 15 M.-T. Chen and C.-T. Chen, *Dalton Trans.*, 2011, **40**, 12886–12894.
- 16 C. Romain, V. Rosa, C. Fliedel, F. Bier, F. Hild, R. Welter, S. Dagonne and T. Aviles, *Dalton Trans.*, 2012, **41**, 3377–3379.
- 17 R. Petrus and P. Sobota, *Organometallics*, 2012, **31**, 4755–4762.
- 18 I. D'Auria, M. Lamberti, M. Mazzeo, S. Milione, G. Roviello and C. Pellicchia, *Chem.-Eur. J.*, 2012, **18**, 2349–2360.
- 19 X. Xu, Y. Chen, G. Zou and J. Sun, *Dalton Trans.*, 2010, **39**, 3952–3958.
- 20 P. J. Bailey, S. T. Liddle and S. Parsons, *Acta Crystallogr., Sect. E: Struct. Rep. Online*, 2001, **57**, o661–o662.
- 21 P. O. Oguadinma and F. Schaper, *Organometallics*, 2009, **28**, 4089–4097.
- 22 M. Stender, R. J. Wright, B. E. Eichler, J. Prust, M. M. Olmstead, H. W. Roesky and P. P. Power, *J. Chem. Soc., Dalton Trans.*, 2001, 3465–3469.
- 23 H. Hamaki, N. Takeda, T. Yamasaki, T. Sasamori and N. Tokitoh, *J. Organomet. Chem.*, 2007, **692**, 44–54.
- 24 S. Brownstein, E. J. Gabe and L. Prasad, *Can. J. Chem.*, 1983, **61**, 1410–1413.
- 25 N. W. Aboeella, B. F. Gherman, L. M. R. Hill, J. T. York, N. Holm, V. G. Young, C. J. Cramer and W. B. Tolman, *J. Am. Chem. Soc.*, 2006, **128**, 3445–3458.
- 26 D. Li, I. Keresztes, R. Hopson and P. G. Williard, *Acc. Chem. Res.*, 2009, **42**, 270–280.
- 27 C. Gallegos, V. Taberero, F. M. García-Valle, M. E. G. Mosquera, T. Cuenca and J. Cano, *Organometallics*, 2013, **32**, 6624–6627.
- 28 A. Macchioni, G. Ciancaleoni, C. Zuccaccia and D. Zuccaccia, *Chem. Soc. Rev.*, 2008, **37**, 479–489.
- 29 J. Gil-Rubio, V. Cámara, D. Bautista and J. Vicente, *Inorg. Chem.*, 2013, **52**, 4071–4083.
- 30 M.-J. Oliva-Madrid, J.-A. García-López, I. Saura-Llamas, D. Bautista and J. Vicente, *Organometallics*, 2014, **33**, 33–39.
- 31 M. J.-L. Tschan, J. Guo, S. K. Raman, E. Brulé, T. Roisnel, M.-N. Ranger, R. Legay, G. Durieux, B. Rigaud and C. M. Thomas, *Dalton Trans.*, 2014, **43**, 4550–4564.
- 32 A. Beitat, S. P. Foxon, C.-C. Brombach, H. Hausmann, F. W. Heinemann, F. Hampel, U. Monkowius, C. Hirtenlehner, G. Knor and S. Schindler, *Dalton Trans.*, 2011, **40**, 5090–5101.
- 33 W. Yang, H. Schmider, Q. Wu, Y.-s. Zhang and S. Wang, *Inorg. Chem.*, 2000, **39**, 2397–2404.
- 34 J. E. Parks and R. H. Holm, *Inorg. Chem.*, 1968, **7**, 1408–1416.
- 35 D. V. Vitanova, F. Hampel and K. C. Hultsch, *J. Organomet. Chem.*, 2005, **690**, 5182–5197.
- 36 G. M. Sheldrick, *SHELXL-97*, University of Göttingen, Germany, 1997.
- 37 *SAINT, Manual Version 5/6.0*, Bruker Analytical X-ray Systems Inc., Madison, WI, 1997.
- 38 *SHELXTL-PC, Manual Version 5.1*, Bruker Analytical X-ray Systems Inc., Madison, WI, 1997.